Magneto-Hydro-Dynamic Waves in the Collisionless Space Plasma

N.S. Dzhalilov [1], V.D. Kuznetsov [2], J. Staude [3]

[1] Shamakhy Astrophysical Observatory (ShAO) named after N.Tusi,

Azerbaijan National Academy of Sciences, Baku, Azerbaijan

e-mail: namigd@mail.ru

[2] Pushkov Institute of Terrestrial Magnetism, Ionosphere and Radio Wave Propagation (IZMIRAN),

Russian Academy of Sciences, Troitsk, Moscow Region, Russia

[3] Astrophysicalisches Institut Potsdam (AIP), Potsdam, Germany

Abstract. The instability of magneto-hydro-dynamic (MHD) waves in an anisotropic, collisionless, rarefied hot plasma is studied. Anisotropy properties of such a plasma are caused by a strong magnetic field, when the thermal gas pressures across and along the field become unequal. Moreover, there appears an anisotropy of the thermal fluxes. The study of the anisotropy features of the plasma are motivated by observed solar coronal data. The 16-moments equations derived from the Boltzmann-Vlasov kinetic equation are used. These equations strongly differ from the usual isotropic MHD case. For linear disturbances the wave equations in homogenous anisotropic plasma are deduced. The general dispersion relation for the incompressible wave modes is derived, solved and analyzed. It is shown that a wide wave spectrum with stable and unstable behavior is possible, in contrast to the usual isotropic MHD case. The dependence of the instability on magnetic field, pressure anisotropy, and heat fluxes is investigated. The general instability condition is obtained. The results can be applied to the theory of solar and stellar coronal heating, to wind models and in other modeling, where the collisionless approximation is valid.

1. Introduction

Since the first identification of the coronal emission lines as forbidden lines of multiply ionized atoms (*Fe, Ni*) by Grotrian [1] and Edlén [2] it has been recognized that the corona has a high temperature of $T > 10^6$ K and requires permanent heating. Heating by acoustic waves was first proposed by Biermann [3]. Later the idea has been extended to magneto-hydro-dynamic (MHD) waves because heating seems to be focused to regions with magnetic field concentrations, to closed fields in particular. Parker [4, 5] suggested heating by currents due to topological dissipation of magnetic fields braided by photospheric footpoint motions. So far a huge number of interesting heating mechanisms have been suggested, but it turned out to be difficult to select and prove the most probable mechanisms by existing observations. Recently, new excellent space-borne data became available; simultaneously the plasma physics simulations and MHD modeling in particular have reached a degree of realism which suggests to look again for a solution of the problem. For example, Aschwanden et al [6] gave 10 arguments against local heating in the corona, but in favor of primary heating in the upper chromosphere and transition region, in the footpoint regions of closed magnetic loops.

Our knowledge of coronal loop oscillations has greatly improved by imaging observations, mainly onboard the SOHO and TRACE satellites [7]. Different kinds of strongly damped oscillation modes are observed as transverse amplitude oscillations with periods of 2 – 30 *min*. By imaging radio measurements modes with much shorter periods are detected. The great variety of waves and oscillations observed in detail in the corona [7, 8] suggests to consider wave heating again. Acoustic waves are damped in the lower chromosphere. MHD waves, transverse incompressible Alfvén waves in particular, can travel along the magnetic field, reach coronal heights and bring enough energy to these heights. However, it is difficult to convert globally this energy into heat. In order to increase the dissipation various mechanisms of damping of such waves have been suggested (see [9]), such as phase mixing, resonant damping, coupling to compressible (slow and fast) MHD modes, and kinetic effects (ion-cyclotron resonance). The coronal emission lines arising practically at all altitudes with different magnetic configurations demonstrate a non-thermal broadening of the profiles. From Doppler shift estimates the amplitudes of such

motions are in the range of 25 – 50 km s^{-1}. The origin of such turbulent motions is unclear.

The coronal plasma is very anisotropic and inhomogeneous, in cross-field direction in particular [7]. Various topologies of a strong magnetic field with open and closed configurations in an almost collisionless, rarefied, hot space plasma lead to its strong anisotropy, and the transport coefficients become tensor quantities. Under such circumstances a traditional hydro-dynamical description of the plasma is impossible. That is why we try to extend the MHD equations by considering the anisotropy of the magnetized collisionless plasma.

Let us consider, for instance, the characteristic parameters of the solar corona: a temperature of $T_e \approx T_i = 10^6$ K, a density of $n_e \approx n_p = 10^9$ cm^{-3} (subscripts e, i, and p mark values for electrons, ions, and protons, respectively), and a range of magnetic field strengths of $B = 0.1 - 100$ G. Using these parameters we get the following estimates: electron and ion thermal velocities of $v_{Te} \approx 4 \times 10^3$ km s^{-1} and $v_{Ti} \approx 100$ km s^{-1}, electron and ion collision times of $\tau_e \approx 10^{-2}$ s and $\tau_i \approx 0.8$ s, electron and ion mean free paths of $\lambda_e \approx 40$ km and $\lambda_i \approx 80$ km, electron and ion gyroradii of $r_{Be} \approx 200 - 0.2$ cm and $r_{Bi} \approx 9000 - 9$ cm, electron and ion gyrotimes of $\tau_{Be} \approx 10^{-6} - 10^{-9}$ s and $\tau_{Bi} \approx 10^{-2} - 10^{-5}$ s, Alfvén and sound speeds of $v_A \approx 10 - 10^4$ km s^{-1} and $c_S \approx 100$ km s^{-1}, respectively. Hence the conditions of a strong magnetic field — $\lambda_e \gg r_{Be}$, $\lambda_i \gg r_{Bi}$, $\tau_e \gg \tau_{Be}$, and $\tau_i \gg \tau_{Bi}$ — are well satisfied. That means, particles gyrating around the magnetic field lines are localized across the field at a distance of the Larmor radius which for motions across the magnetic field plays the role of a free path length of particles. Thus the dynamical motion of a collisionless plasma with characteristic scales of L $\gg$ r_B and $\tau \gg \tau_B$ behaves across the magnetic field as a fluid.

Frequent collisions turn the plasma distribution function to an isotropic one, and thus the thermal pressure is isotropic as well. If collisions rarely occur, the energies of chaotic motions are no longer "mixed", and pressure becomes anisotropic. The presence of a magnetic field will maintain a "non-mixed" state of the energies of longitudinal and transverse motions of particles. So, the transverse and longitudinal pressures will differ from each other, $\alpha = p_\perp / p_\parallel = \overline{T}_\perp / \overline{T}_\parallel \neq 1$ (here p and $\overline{T}$ are the mean thermal pressure and temperature). For a very short time τ_{Be} across the magnetic field mean values of thermal pressure and temperature are established, but this does not occur so fast along the field. As a result the plasma becomes colder along the magnetic field, $T_\parallel < T_\perp$. A distinct thermal anisotropy of $T_\perp / T_\parallel \sim 2 - 3$ has been observed in the solar wind, see for example, Feldman et al [10], Marsch et al [11], and Casper et al [12]. A strong anisotropy of temperature of the ionospheric plasma

reaching 50-60 percent is really found in experiments, see Clark et al [13] and Likhter et al [14]. Large heavy-ion thermal anisotropies ($T_\perp / T_\parallel > 100$) were also detected in the solar corona by UVCS/SoHO by Kohl et al [15] and Cranmer et al [16]. A similar but smaller anisotropy exists for protons, see Cranmer et al [16], and for the coronal hole temperature anisotropy, see Dodero et al [17] and Antonucci et al [18]. It is now generally accepted that the observed large ion temperature anisotropies are related to the physical mechanism by which the solar corona and solar wind are heated, see Hollweg and Isenberg [19], and Marsch [20].

Along the magnetic field the plasma is collisionless, if the particle parallel mean free path is not small in comparison with the considered characteristic scales: $\lambda_{e,i} \approx 50$ km, so that the wavelength along the magnetic field is $\lambda_\parallel < 50$ km. The hydro-dynamical description can also be applied to the motions of such a plasma. The criterion of applicability of the hydro-dynamical description in this case is obtained by comparing self-consistently the electric force with the pressure gradient; it is connected with the smaller thermal velocity of particles in comparison with the speeds of the directed stream: $\alpha^{-1/2} v_T < v_0 \sim v_A$, see Oraevskii et al [21].

Due to the anisotropy of the kinematic temperatures of protons and heavy ions the corresponding partial pressures become anisotropic in this way. This makes the total thermal pressure anisotropic too, $p_\perp \neq p_\parallel$. Physically such a situation can be realized only if the particle collisions in the plasma are rare. In the present paper we consider the wave peculiarities which can appear in a collisionless plasma. With this objective we formulate in Section 2 the basic equations, which are the integrated moments' equations of the kinetic Boltzmann-Vlasov equation. In Section 3 the linear wave equation and the general dispersion relation for the incompressible case are derived. The solutions and analyzes of the dispersion equation are the topic of Section 4. In Section 5 we investigate the instability domains in dependence on the magnetic field, on the pressure anisotropy parameter, and on thermal fluxes. The discussion and conclusions are presented in Section 6. In the Appendix the common expression describing the boundaries of the instability domains is derived.

2. Basic Equations

A successful way to describe a plasma is the use of the system of the equations consisting of the kinetic equations for the distribution functions of the particles and the Maxwell equations for the electromagnetic field. The hydro-dynamical approach is based on the isotropic character of the distribution of the degrees of freedom of thermal energy for the plasma components in the form of (or very close to) the Maxwell function. However, in real situations the distribution functions of the space plasma components, ions in particular, differ strongly from the Maxwell function.

Despite the relative smallness of $\lambda_{e,i} / \lambda_T \ll 1$ (λ_T is the thermal scale height), the coronal plasma, for example,

cannot be described satisfactory by theories supposing that local velocity distribution functions are close to Maxwellians, see Marsch [20].

The distribution function $f_a(\vec{u}, \vec{r}, t)$ describes the density of particles of a kind a in the six-dimensional phase space $(\vec{u}, \vec{r})$; it is the solution of the kinetic Boltzmann-Vlasov equation:

$$\frac{\partial f_a}{\partial t} + \vec{u}_a \nabla f_a + \frac{1}{m_a}\left\{\vec{F}_a + e_a\left(\vec{E} + \frac{1}{c}\left[\vec{u}_a \vec{B}\right]\right)\right\}\nabla_u f_a = Q_a \quad (1).$$

Here $\vec{E}$ and $\vec{B}$ are the total electric and magnetic fields, e_a and m_a are the charge and mass of particles of a sort a, $\vec{F}_a$ are the non-electromagnetic forces; c is the speed of light, ∇_u is the gradient in the velocity space, and $Q_a(f_a)$ are the integrals of collisions. This statistical equation for the plasma is deduced assuming that the ratio of the average energy of the interaction of two particles to their average kinetic energy is small enough. That means the number of particles in a plasma sphere with a Debye radius r_D should be $\bar{g} = 1/nr_D^3 \ll 1$. In a collisionless approach $Q_a = 0$. The left-hand part of Eq. (1) gives an effect of the order of unity, while the right-hand part for pair collisions (Landau integrals of collisions), for example, gives an effect of order $\bar{g}$ [22]. For coronal conditions $\bar{g} \approx 10^{-6}$, hence the collisionless approach can be applied. All the macroscopic parameters (density, plasma flow speed, pressure, thermal flux, tensor of viscosity, etc.) are defined as the corresponding speed moments of the distribution function:

$$M^{(k)} = M^{(k)}_{\alpha 1...\alpha k}(\vec{r},t) = \int\prod_{j=1}^{k}u_{a,j}f d\vec{v} \ , \ \alpha_i = 1,2,3.$$

For example, the density of particles is $n = n(\vec{r},t) = \int f \, d\vec{u}$, the hydro-dynamical speed of the plasma is $n\vec{v}(\vec{r},t) = \int \vec{u} f \, d\vec{u}$, where $d\vec{u} = du_x du_y du_z$. Due to the complexity of Eq. (1), usually the equations for the moments of the distribution function are deduced, and these equations refer to the hydro-dynamical or the transport equations. The main difficulty in deducing these transport equations consists in the problem that in the infinite chain the momentum equations become coupled among each other, therefore some additional physically proved assumptions for truncating this chain are required.

In a collision dominated plasma one can decompose the distribution functions around the basic state of an isotropic equilibrium which is described by the Maxwell function, and if hydrodynamics can be applied a truncation of the chain of moment equations leads to rather simple MHD equations. If collisions among particles are rare and a strong magnetic field is present, the conditions become more complicated, however, for a collisionless plasma mainly across a magnetic field the hydro-dynamical approach can be used, see, e.g., Chew et al [23], and Rudakov and Sagdeev [24]. In this approximation the distribution function in a strong

external magnetic field will depend on both speeds, those along and across the field: $f(\vec{r}, \vec{u}, t) \rightarrow f(\vec{r}, \vec{u}_{\parallel}, \vec{u}_{\perp}, t)$.

The solution of the kinetic equations is searched for in the form of the expansion

$$f(\vec{u}, r, t) = f_0(\vec{u}, r, t)\sum_{k,v} a_v(\vec{r}, t)P_v^{(k)}(\vec{u}, r, t), \quad (2)$$

where f_0 is the weighting function of the expansion (the zero-approach distribution function), a_v are the expansion coefficients, v are the coordinates, $P^{(k)}$ is an orthogonal polynomial of order k (for example, a Hermitian polynomial). If a Maxwellian distribution is chosen for the weight function f_0, Eq. (2) describes a state close to the thermodynamic equilibrium. Such an approach refers to the method of Grad [25]. However, the method of Grad cannot be applied to describe a plasma with arbitrary anisotropic pressure. For this purpose Oraevskii et al [26, 21] have used a bi-Maxwellian quasi-equilibrium distribution,

$$f_0 = n\left(\frac{m}{2\pi kT_{\perp}}\right)\left(\frac{m}{2\pi kT_{\parallel}}\right)^{1/2}\exp\left(-\frac{mu_{\perp}^2}{2kT_{\perp}} - \frac{mu_{\parallel}^2}{2kT_{\parallel}}\right). \quad (3)$$

For a small parameter $\bar{g} \rightarrow 0$ the plasma is closer to a thermo-dynamical equilibrium state. In that case the multi-partial distribution function is close to a product of single partial distribution functions [22]. Therefore it is justified to use a bi-Maxwellian distribution calculated by multiplying the two functions along the magnetic field and across the field. This method introduces two vectors of thermal fluxes, and the total distribution function is expressed through 16-moments. The method of Grad results in 13–moments equations. The conditions for truncating the chain of the equations to the 16–moments equations are reduced to the following two statements:

a) the components of the viscosity tensor should be much smaller than the pressures across and along the field, $p_{\perp}, p_{\parallel}$;

b) thermal fluxes $S_{\perp}, S_{\parallel} \ll \rho v_T^3$, where $v_T = \sqrt{kT/m}$ is the thermal speed.

These requirements are satisfied in the transverse direction, if $r_B/L_{\perp} \ll 1$, $\tau_B/\tau \ll 1$. In the longitudinal direction we should have $a_{II} = v_{T\parallel}\tau/L_{\parallel} \ll 1$. $a_{\parallel} \rightarrow 0$ means small pressure forces (thermal motion of particles) in comparison with the electromagnetic forces, i.e. the plasma is "cold". In this case the equation of motion is transformed into the equations of motion for the separate components of the plasma.

The 16–moments set of equations was used by many authors in different theoretical approaches, especially for modeling the solar wind, see Demars and Schunk [27], Olsen and Leer [28], Li [29], and Lie-Svendsen et al [30]. Thus, the 16–moments set of transport or MHD (not in the sense of the usual isotropic case) equations for the collisionless plasma in the presence of gravity g but

without magnetic diffusivity under the conditions of $\tau_B \ll V\tau$, $\tau_B \ll v_T\tau$ is given as follows, see Oraevskii et al [21]:

$$\frac{d\rho}{dt} + \rho\, divv = 0, \tag{4}$$

$$\rho\frac{d\vec{v}}{dt} + \nabla\left(p_\perp + \frac{B^2}{8\pi}\right) - \frac{1}{4\pi}(\vec{B}\cdot\nabla)\vec{B} = \rho\,\vec{g} + \tag{5}$$

$$+ (p_\perp - p_\parallel)[\vec{h}\,div\vec{h} + (\vec{h}\cdot\nabla)\vec{h}] + \vec{h}(\vec{h}\cdot\nabla)(p_\perp - p_\parallel),$$

$$\frac{d}{dt}\frac{p_\parallel B^2}{\rho^3} = -\frac{B^2}{\rho^3}\left[B(\vec{h}\cdot\nabla)\left(\frac{S_\parallel}{B}\right) + \frac{2S_\perp}{B}(\vec{h}\cdot\nabla)B\right], \tag{6}$$

$$\frac{d}{dt}\frac{p_\perp}{\rho B} = -\frac{B}{\rho}(\vec{h}\cdot\nabla)\left(\frac{S_\perp}{B^2}\right), \tag{7}$$

$$\frac{d}{dt}\frac{S_\parallel B^3}{\rho^4} = -\frac{3p_\parallel B^3}{\rho^4}(\vec{h}\cdot\nabla)\left(\frac{p_\parallel}{\rho}\right), \tag{8}$$

$$\frac{d}{dt}\frac{S_\perp}{\rho^2} = -\frac{p_\parallel}{\rho^2}\left[(\vec{h}\cdot\nabla)\left(\frac{p_\perp}{\rho}\right) + \frac{p_\perp}{\rho}\frac{p_\perp - p_\parallel}{p_\parallel B}(\vec{h}\cdot\nabla)B\right], \tag{9}$$

$$\frac{d\vec{B}}{dt} + \vec{B}\,div\vec{v} - (\vec{B}\cdot\nabla)\vec{v} = 0, \quad div\vec{B} = 0, \tag{10}$$

where $\nabla = \nabla_\parallel + \nabla_\perp$, $\nabla_\parallel = \vec{h}(\vec{h}\cdot\nabla)$, and

$$\frac{d}{dt} = \frac{\partial}{\partial t} + (v\cdot\nabla), \quad v = v_\parallel + v_\perp, \quad \vec{h} = \frac{\vec{B}}{B} \tag{11}$$

Here $\mathbf{S}_\parallel$ and $S_\perp$ are the heat fluxes along the magnetic field by parallel and perpendicular thermal motions. If the thermal fluxes are neglected, $S_\perp = 0$ and $\mathbf{S}_\parallel = 0$, we receive the equations describing the laws of the change of longitudinal and transverse thermal energy along the trajectories of the plasma (the left-hand parts of Eqs. (6) and (7). These so-called "double-adiabatic" parities and Eqs. (4), (5), and (10) form as though a closed system of equations, the CGL (Chew-Goldberger-Low) equations, see Chew et al [23]. However, using the CGL-equations can result in unsatisfactory Eqs. (8, 9). This is because deducing the CGL equations the third moments of the distribution function, hence the thermal fluxes, have been lost without any proof, see Chew et al [23], and Baranov and Krasnobayev [31]. The equations following from the 16–moments set in our case, Eqs. (4 - 10), consider the thermal fluxes, they are more complete, and the CGL equations do not follow from these equations as a special case. One should compare the final results in the limits $S_\perp \to 0$ and $S_\parallel \to 0$ with the results based on the CGL equations, deduced by many authors, see, e.g., Kato et al [32], Baranov and Krasnobayev [31], and Kuznetsov and Oraevskii [33].

3. Wave equations

For simplicity we will now assume, that the basic initial equilibrium state of the plasma is homogeneous, $g = 0$, and the following quantities are constant: $v_0, \rho_0, p_{\perp o}, p_{\parallel 0}, B_0, S_{\perp 0},$ and $S_{\parallel 0}$. Eqs. (4–10) will automatically satisfy such an equilibrium state with non-

zero thermal fluxes. We will consider small linear perturbations of all physical variables, e.g. for pressure in the form $p = p_0 + p'(r,t)$.

Let $p'(r,t) \sim \exp i(\vec{k}\cdot\vec{r} - \omega t)$, where $\omega = \omega_0 + (\vec{v}_0\cdot\vec{k})$ is the wave frequency observed in the moving frame of the fluid, and k is the wave number of the fluctuations. For the perturbations we receive the equations

$$\omega\rho' - \rho_0(\vec{k}\cdot\vec{v}) = 0 \tag{12}$$

$$\omega\rho_0\vec{v} - \vec{k}\left(p_\perp' + \frac{\vec{B}_0\cdot\vec{B}'}{4\pi}\right) + k_*\frac{B_0}{4\pi}\vec{B}' - \tag{13}$$

$$- \Delta[\vec{h}_0(\vec{k}\cdot\vec{h}') + k_*\vec{h}'] - k_*\vec{h}_0(p_\parallel' - p_\perp') = 0,$$

$$\omega\vec{B}' - \vec{B}_0(\vec{k}\cdot\vec{v}) + (\vec{k}\cdot\vec{B}_0)\vec{v} = 0, \quad (\vec{k}\cdot\vec{B}') = 0, \tag{14}$$

$$a_0\frac{p_\perp'}{p_{\perp 0}} = a_1\frac{B'}{B_0} + a_2\frac{\rho'}{\rho_0}, \tag{15}$$

$$b_0\frac{p_\parallel'}{p_{\parallel 0}} = b_1\frac{B'}{B_0} + b_2\frac{\rho'}{\rho_0}. \tag{16}$$

Deriving these equations we have excluded fluctuations of the thermal fluxes, using

$$S_\perp' = \frac{k_*p_{\parallel 0}p_{\perp 0}}{\omega\rho_0}\left[\frac{p_\perp'}{p_{\perp 0}} - \frac{\rho'}{\rho_0} - \frac{\Delta}{p_{\parallel 0}}\frac{B'}{B_0}\right] + 2S_{\perp 0}\frac{\rho'}{\rho_0}, \tag{17}$$

$$S_\parallel' = \frac{3p_{\parallel 0}^2 k_*}{\rho_0\omega}\left(\frac{p_\parallel'}{p_{\parallel 0}} - \frac{\rho'}{\rho_0}\right) - S_{\parallel 0}\left(\frac{3B'}{B_0} - 4\frac{\rho'}{\rho_0}\right). \tag{18}$$

Here $\Delta = p_{\parallel 0} - p_{\perp 0}$, $\vec{h}_0 = \vec{B}_0/B_0$, $k_* = (h_0\cdot k) = k\cos\phi$. The indices II and $\perp$ correspond to the values of the parameters along and across the magnetic field. Even if we insert in Eqs. (17–18) $S_{\parallel 0} = S_{\perp 0} = 0$, the perturbations of these functions will never become zero: $S_\parallel' \neq 0$, $S_\perp' \neq 0$. That means, using the 16–moments equations we should get more reliable results on the wave properties in an anisotropic plasma than with the CGL equations based on the 13–moments equations.

Strictly speaking, the heat fluxes of particles of a kind a should be defined as $\vec{S}_a = n_a m_a\langle\frac{1}{2}c_a^2\vec{c}_a\rangle$, where $\vec{c}_a = \vec{u} - \vec{v}_a$ is the chaotic thermal speed. In the presence of an external magnetic field the components of this flux are defined by the solutions of the kinetic Eq. (1). However, we should use here some appropriate estimate as a parameter.

The initial collisionless heat flux functions $S_{\parallel 0}$ and $S_{\perp 0}$ should be estimated by taking the thermal energy density of the electrons multiplied by the non-thermal flow speed along the magnetic field v_0:

$$S_{\parallel 0} \approx \frac{3}{2}n_e k_B T_\parallel v_0 \delta = \frac{3}{4}\delta v_0 p_\parallel.$$

Hollweg [34, 35] has given some estimates of the correction parameter δ (α in his papers) assuming various realistic shapes of the electron distribution function in Eq. (1) and checking the results for

agreement with space observations. δ depends on the magnetic field. In the range of $B = 0.1 - 100$ G we have $\delta \approx 4-0.1$. In the same way $S_{\perp 0} \approx \frac{3}{4} \delta v_0 p_\perp$. Using the condition $S_{\parallel,\perp} << \rho (v_T)^3_{\parallel,\perp}$ mentioned above, we get some restriction for v_0: $\delta c_s^2 v_0 << v_{Te}^3$. Even for the maximum Alfvén velocity $v_0 \approx v_A$ this condition is obeyed. For coronal conditions we should identify v_0 with the observed non-thermal velocities which follows from the broadening of spectral lines: $\sim 30 - 50 \ km \ s^{-1}$.

Let us introduce dimensionless parameters (in the further text indexes "0" of physical parameters will be omitted for simplicity):

$$\alpha = \frac{p_\perp}{p_\parallel}, \ \overline{\alpha} = 1-\alpha, \ c_\parallel^2 = \frac{p_\parallel}{\rho},$$

$$\beta = \frac{B^2}{4\pi p_\parallel} = \frac{v_A^2}{c_\parallel^2}, \ \eta = \frac{c_\parallel k_\parallel}{\omega} = \frac{c_\parallel k}{\omega} \cos \phi, \quad (19)$$

$$\overline{S}_\parallel = \frac{S_\parallel}{p_\parallel c_\parallel}, \ \overline{S}_\perp = \frac{S_\perp}{p_\perp c_\parallel},$$

$$\overline{S} = \alpha \overline{S}_\perp - 2\overline{S}_\parallel, l_1 = \cos^2 \phi, l_2 = \sin^2 \phi \quad (20)$$

Note that β is defined here inversely proportional to the often used "plasma beta". By means of these parameters the coefficients $a_{0,1,2}$ and $b_{0,1,2}$ are defined as

$$a_0 = 1-\eta^2, \quad a_1 = 1 - 2\overline{S}_\perp \eta - \overline{\alpha} \eta^2, \quad (21)$$

$$a_2 = 1 + 2\overline{S}_\perp \eta - \eta^2, \quad (22)$$

$$b_0 = 1-3\eta^2, b_1 = 2\eta \overline{S}, b_2 = 3 + 4\overline{S}_\parallel \eta - 3\eta^2. \quad (23)$$

Having excluded ρ' and P' from Eqs. (12-16) we receive

$$\frac{1}{\eta} \frac{v}{c_\parallel} - \alpha \frac{\vec{k}}{k_*} \left(\frac{a_1}{a_0} \frac{B'}{B} + \frac{a_2}{a_0} \frac{(\vec{k} \cdot \vec{v})}{\omega} + \frac{(\vec{B} \cdot \vec{B'})}{4\pi p_\perp} \right) +$$

$$+ \frac{\vec{B'}}{B} (\beta - \overline{\alpha}) - \frac{\vec{B}}{B} \left[\left(\frac{b_1}{b_0} - \alpha \frac{a_1}{a_0} - 2\overline{\alpha} \right) \frac{B'}{B} + \left(\frac{b_2}{b_0} - \alpha \frac{a_2}{a_0} \right) \frac{(\vec{k} \cdot \vec{v})}{\omega} \right] = 0, \quad (24)$$

$$\frac{\vec{B'}}{B} - \frac{\vec{B}}{B} \frac{(\vec{k} \cdot \vec{v})}{\omega} + \frac{k_*}{\omega} \vec{v} = 0, \ (\vec{k} \cdot \vec{B'}) = 0. \quad (25)$$

The $\vec{k}$- and $\vec{B}$-components of these vector equations are given by

$$\left(\frac{1}{\eta^2} - \frac{\alpha l_2}{l_1} \frac{a_2}{a_0} - \frac{b_2}{b_0} \right) \frac{(\vec{k} \cdot \vec{v})}{\omega} - \frac{1}{l_1} \frac{\vec{B} \cdot \vec{B'}}{4\pi p_\parallel} -$$

$$- \left(\frac{\alpha l_2}{l_1} \frac{a_2}{a_0} + \frac{b_1}{b_0} - 2\overline{\alpha} \right) \frac{B'}{B} = 0, \quad (26)$$

$$\frac{1}{\eta} \frac{(\vec{B} \cdot \vec{v})}{Bc_\parallel} - \frac{b_2}{b_0} \frac{(\vec{k} \cdot \vec{v})}{\omega} - \overline{\alpha} \frac{(\vec{B} \cdot \vec{B'})}{B^2} - \left(\frac{b_1}{b_0} - 2\overline{\alpha} \right) \frac{B'}{B} = 0, \quad (27)$$

$$\eta \frac{(\vec{B} \cdot \vec{v})}{Bc_\parallel} - \frac{(\vec{k} \cdot \vec{v})}{\omega} + \frac{(\vec{B} \cdot \vec{B'})}{B^2} = 0, (\vec{k} \cdot \vec{B'}) = 0. \quad (28)$$

In analogy to usual MHD as used by Somov et al [36], there are two independent wave branches in the plasma: waves which do not compress the plasma ($div \vec{v} = 0$), and waves compressing the plasma ($div \vec{v} \neq 0$). In this paper we shall restrict ourselves to the wave modes uncompressing the plasma.

Having inserted in Eqs. (26–28) the condition of incompressibility $(\vec{k} \cdot \vec{v}) = 0$, and excluded the variables $(\vec{B} \cdot \vec{v})$ and $(\vec{B} \cdot \vec{B'})$ we receive
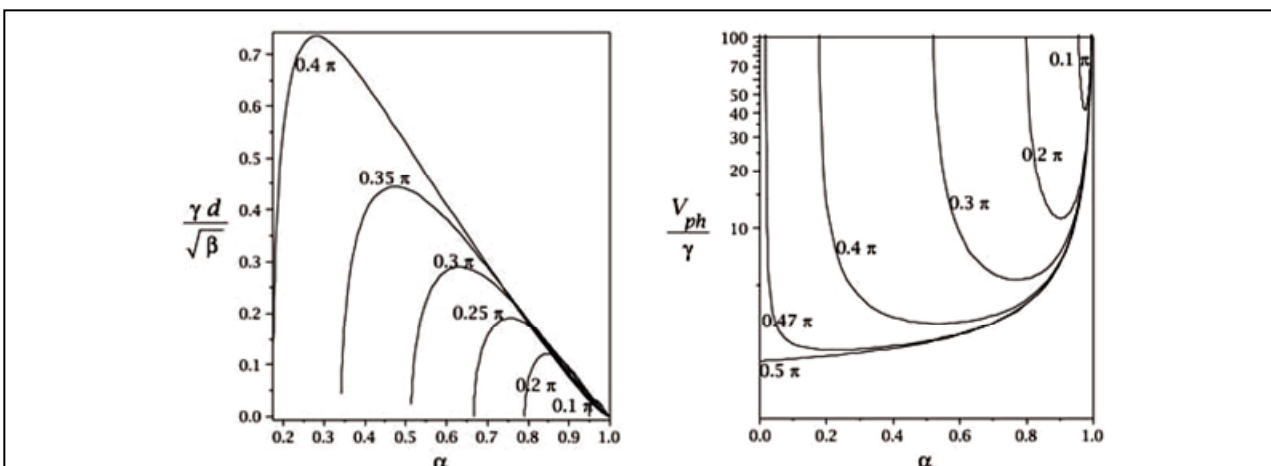

Fig. 1. Increment/decrement of the instability normalized to $\sqrt{\beta}/\gamma$ as a function of the anisotropy parameter α in the domain of the instability (left picture). In the right picture the phase velocity of the unstable modes $V_{ph} = R_{e\omega}/k_\parallel c_\parallel$ normalized to γ is shown. The numbers on the curves are values of the propagation angle ϕ. These figures are asymptotic $\beta \to \infty$ limit cases of unstable solution of Eq. (31).

$$\left[\alpha\frac{a_1}{a_0}+l_1\left(\frac{b_1}{b_0}-\alpha\frac{a_1}{a_0}-2\overline{\alpha}\right)\right]\left(\frac{1}{\eta^2}+\overline{\alpha}\right)\frac{B'}{B}- \tag{29}$$

$$-\beta\left(\frac{b_1}{b_0}-2\overline{\alpha}\right)\frac{B'}{B}=0.$$

As far as $B'\neq0$ the dispersion relation must be fulfilled:

$$\left[\alpha\frac{a_1}{a_0}+l_1\left(\frac{b_1}{b_0}-\alpha\frac{a_1}{a_0}-2\overline{\alpha}\right)\right]\left(\frac{1}{\eta^2}+\overline{\alpha}\right)--\beta\left(\frac{b_1}{b_0}-2\overline{\alpha}\right)=0. \tag{30}$$

This is a polynomial equation of 6th order in the frequency of the fluctuations. For the parameter $Z=1/\eta=\omega/\left(c_{\parallel}k_{\parallel}\right)$ this equation can be written in the form

$$c_6Z^6+c_5Z^5+c_4Z^4+c_3Z^3+c_2Z^2+c_1Z+c_0=0, \tag{31}$$

where

$$c_0=3\overline{\alpha}\left[\beta+\overline{\alpha}\left(\alpha l_2/2-l_1\right)\right],$$
$$c_1=\overline{\alpha}\gamma\left[3\alpha l_2-l_1(\alpha-2)\right]+\beta\gamma(\alpha-2),$$
$$c_2=\overline{\alpha}\left(4\alpha l_1-3l_1-\overline{\alpha}\alpha l_2/2-4\beta\right),$$
$$c_3=\gamma\left[3\alpha l_2-(l_1+\beta)(\alpha-2)+\overline{\alpha}\left(l_1(\alpha-2)-\alpha l_2\right)\right],$$
$$c_4=\overline{\alpha}\left(\beta-\overline{\alpha}l_1+4l_1\right)-3\alpha l_2/2,$$
$$c_5=\gamma\left[l_1(\alpha-2)-\alpha l_2\right],\ c_6=\alpha l_2/2-\overline{\alpha}l_1$$

Here the dimensionless parameter $\gamma=(3/4)\delta v_0/c_{\parallel}$ is introduced, by which the heat fluxes are defined: $\overline{S}_{\parallel}=\overline{S}_{\perp}=\gamma$, $\overline{S}=\gamma(\alpha-2)$. In the usual isotropic MHD case only the Alfvén waves with $\omega^2=k_{\parallel}^2v_A^2$ can arise, the phase velocities of which are equal to each other in both directions with respect to the magnetic field. So, instead of $Z^2=\beta$ in the isotropic MHD we have deduced now the 6-th order Eq. (32) in the anisotropic MHD. With the non-zero heat fluxes $\gamma\neq0$, odd non-zero

coefficients c_1,c_3,c_5 will result in wave propagation velocities depending on the direction of the magnetic field. We can expect prograde and retrograde wave modes. Let us first consider the most important limit cases of Eq. (32) which can be solved analytically.

4. Limit cases
4.1. Strong magnetic field

Let us consider the case $v_a^2>>c_{\parallel}^2$ or the limit $\beta\rightarrow\infty$. Using the usual asymptotic expansion we find the six solutions of Eq. (31):

$$Z_{1,2}\approx\beta^{1/2}\left[\pm i\sqrt{\frac{1-\alpha}{c_6}}-\frac{1}{2\sqrt{\beta}}\left(\frac{c_5}{c_6}-\gamma\frac{\alpha-2}{\alpha-1}\right)\right] \tag{32}$$

Here $\alpha\neq1$ and $c_6\neq0$ should be obeyed. In the case $\alpha>>1$ we have $Z^2\approx2\beta/\left(1+\cos^2\phi\right)$.

That means, $\omega^2\approx k_{\parallel}^2v_A^2$ along the magnetic field, $\phi\rightarrow0$, and $\omega^2\approx2k_{\parallel}^2v_A^2$ across the magnetic field, $\phi\rightarrow\pi/2$. In the opposite case $\alpha<<1$ we get an analogy to the inclined Alfvén waves, $\omega^2\approx k^2v_A^2$. So, the solution (32) describes the prototype of the usual (isotropic) Alfvén waves. But for more realistic values of the anisotropy parameter $\alpha\sim O(1)$ these mode becomes unstable. The instability condition is

$$\frac{2\cos^2\phi}{1+\cos^2\phi}<\alpha<1 \tag{33}$$

Instability does not arise for waves propagating along the magnetic field, $\phi=0$. The growing time increases with the magnetic field and does not depend on γ. The second term in Eq. (32) defines the phase velocity of the unstable modes, which is independent from the magnetic field, but it depends strongly on γ. The instability increment and the phase velocity are defined
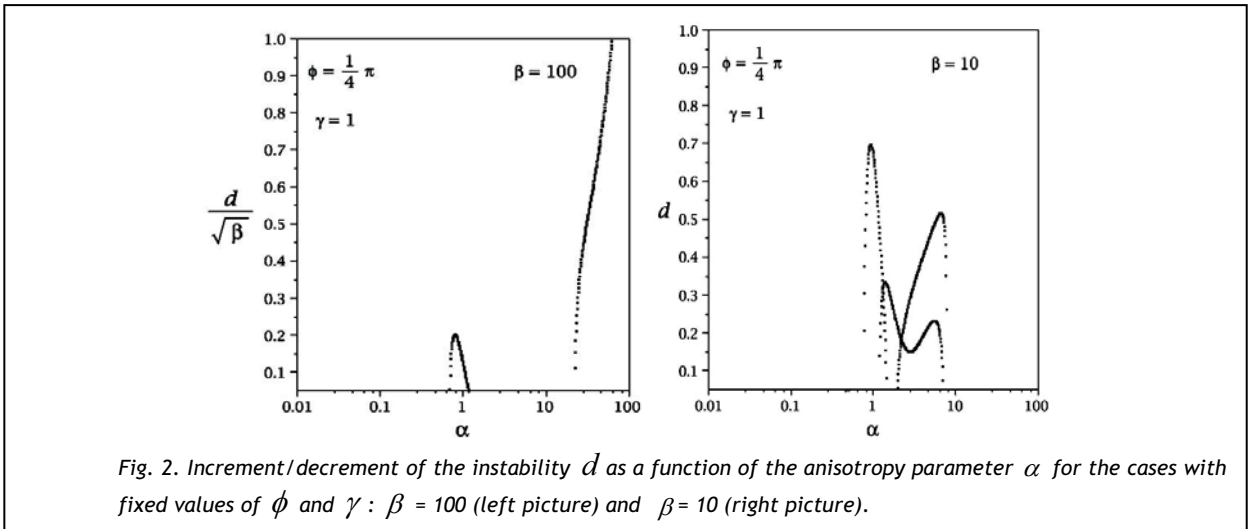

Fig. 2. Increment/decrement of the instability d as a function of the anisotropy parameter α for the cases with fixed values of ϕ and γ: β = 100 (left picture) and β = 10 (right picture).
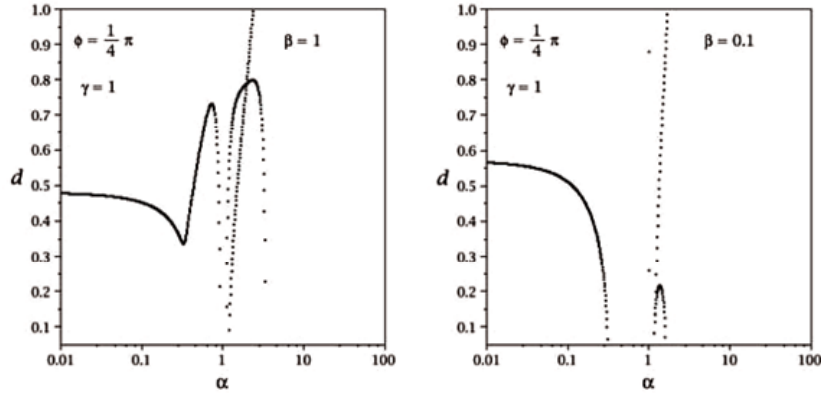
Fig. 3. Increment/decrement of the instability d as a function of the anisotropy parameter α for the cases with fixed values of γ and β: $\beta = 1$ (left picture) and $\beta = 0.1$ (right picture).

Fig. 4. Two characteristic cases of phase velocity $V_{hp} = \mathrm{Re}(\omega)/k_\parallel c_\parallel$ as a function of the anisotropy parameter α for the cases with fixed values of γ and β: $\beta = 1$ (left picture) and $\beta = 100$ (right picture).
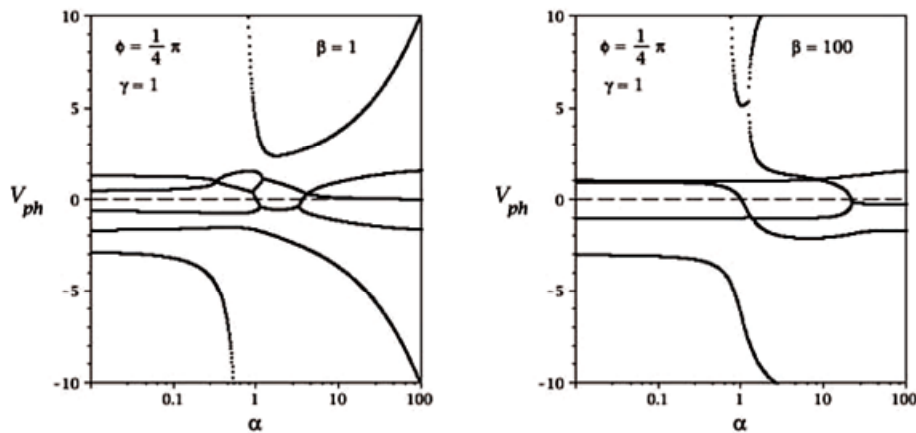
as

$$d = \frac{\mathrm{Im}(\omega)}{\mathrm{Re}(\omega)} = 4\sqrt{\beta c_6(1-\alpha)}\,\frac{1-\alpha}{\gamma\alpha l_2(4-3\alpha)},$$

$$V_{ph} = \frac{\mathrm{Re}(\omega)}{k_\parallel c_\parallel} = \frac{\gamma\alpha l_2(4-3\alpha)}{4c_6(1-\alpha)}. \tag{34}$$

d has both signs and $V_{ph} > 0$, the unstable modes are running along the magnetic field. In Figs. 1 these parameters are shown in the instability range of α. The instability growing increment (or damping decrement) has rather high values. The maxima of d correspond to the minima of the phase velocities. For more inclined modes d becomes larger and the minima of V_{ph} decrease. From the figures for different values of β and γ the increments and phase velocities can easily be estimated.

The other solutions of Eq. (31) present stable waves, $\mathrm{Im}(\omega) = 0$: $Z_{3,4} \approx \pm 1$,

$$Z_{5,6} \approx \frac{\gamma(\alpha-2)\pm\sqrt{\gamma^2(\alpha-2)^2+12(1-\alpha)^2}}{2(1-\alpha)} \tag{35}$$

The first one is practically a symmetric slow wave with $V_{hp} \approx c_\parallel \ll v_A$. The second solutions are strongly asymmetric stable waves, $V_{hp} > 0$ means prograde waves, $V_{hp} < 0$ retrograde waves. For $\alpha < 1$ we have $Z_5 > 0$, that means prograde waves, and $Z_6 < 0$ retrograde ones. In this case $|Z_6| > |Z_5|$, that means retrograde waves are faster. For $\alpha > 1$ we get the opposite case: $Z_5 < 0$ and $Z_6 > 0$. In the range $1 < \alpha < 2$ prograde waves are faster, $|Z_6| > |Z_5|$, and for $\alpha > 2$ we have $|Z_5| > |Z_6|$. $\alpha = 2$ is a symmetric case, $|Z_5| = |Z_6|$. Anti-symmetric features of waves are due to thermal fluxes. If the thermal fluxes are not included, $\gamma = 0$, both waves have the same velocities, such as in the isotropic case. We found analytically the asymptotic solutions of Eq. (31) for $\beta \to \infty$. In this case only one pair of solutions is complex and can become unstable.
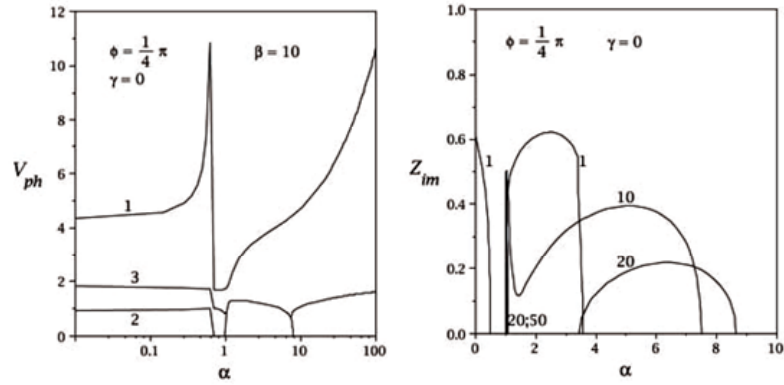
Fig. 5. Absence of thermal fluxes, $\gamma = 0$. The left picture is the phase velocity $V_{ph} = Re(Z)$ as a function of the anisotropy parameter α for the cases of fixed values ϕ and β. The numbers 1, 2, 3 on the curves correspond to the solutions $\zeta_{1,2,3}$. The right picture is the instability increment rate $Z_{im} = Im(Z)$ for different values of β given on the curves.
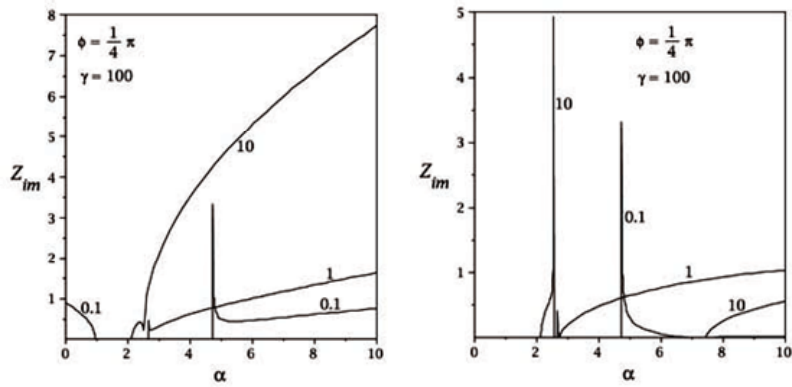

Fig. 6. The case of large thermal fluxes, $\gamma = 100$, where the instability growing rate $Z_{im} = Im(Z)$ in dependence on the anisotropy parameter α is shown. The left and right pictures correspond to the first and second solutions of Eqs. (38), respectively. The numbers on the curves are the values of β.
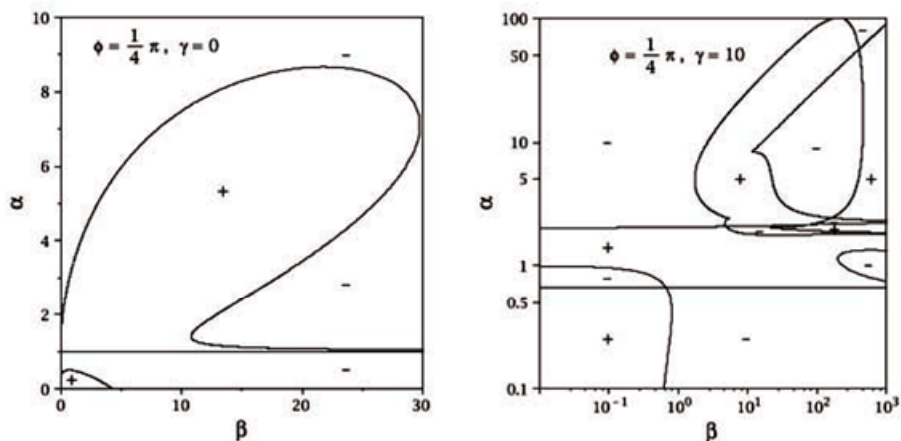

Fig. 7. Instability domain boundaries in the (α, β) plane for fixed values of ϕ and γ. In the curves $Im(\omega) = 0$, these values are found as roots of Eq. (A.5). In the areas labeled with the mark "+" waves are unstable, and with "-" stable.

Let us take from Figs. 1 one characteristic case, say $\phi = 0.25\pi$ and $\gamma = 1$. For this case the exact numerical solutions of Eq. (31) can be found. The cases β = 100, 10, 1, and 0.1 are demonstrated in Figs. 2 and 3, where the increments of the unstable waves are shown.

For moderate values of β all the solutions become complex. For $\beta > 300$ the picture of instability tends to the asymptotic case as shown in Fig. 1. In these figures we see only three roots of the polynomial equation. The other three roots are symmetric with negative sign. Two characteristic cases of phase velocities are shown in Figs. 4. For small and large values of α the solutions are more symmetric, prograde and retrograde modes have more or less the same velocities. Waves with $|V_{ph}| \approx 1$ practically exist in all cases. A more complicated case is the range $1 < \alpha < 2$, where the anisotropy of the modes is strong. An anisotropic propagation of waves is a consequence of the thermal fluxes. Let us consider the two limit cases, $\gamma \to 0$ and $\gamma \to \infty$, analytically.

4.2. Special case $\gamma \to 0$

Although the absence of fluxes, $S_\perp = 0$ and $S_\parallel = 0$, is far from reality, this simplified case has been investigated by other authors using the 13–moments equations. Putting $\gamma = 0$ into Eq. (31) we receive a cubic equation for $\zeta = Z^2$:

$$c_6\zeta^3 + c_4\zeta^2 + c_2\zeta + c_0 = 0 \qquad (36)$$

So we have only symmetric solutions, $Z = \pm\sqrt{\zeta}$:

$$\zeta_1 = s_1 + s_2 - \frac{g_2}{3},$$

$$\zeta_{2,3} = -\frac{1}{2}(s_1 + s_2) - \frac{g_2}{3} \pm i\frac{\sqrt{3}}{2}(s_1 - s_2). \qquad (37)$$

Here $s_{1,2} = \left(r \pm \sqrt{\omega}\right)^{1/3}$, $\omega = q^3 + r^2$, $q = g_1/3 - g_2^2/9$,

$r = (g_1 g_2 - 3g_0)/6 - g_2^3/27$,

$g_2 = c_4/c_6$, $g_1 = c_2/c_6$, $g_0 = c_0/c_6$.

The analytical solutions ζ_1, ζ_2, and ζ_3 allow to investigate them in more detail in dependence on the parameters α, β, and ϕ. For low values of β ζ_1 is real and positive, but the $\zeta_{2,3}$ values are complex conjugate functions. Some characteristic cases are shown in Figs. 5. For small $\beta \leq 1$ there appear two ranges of α, where the waves become unstable, $\text{Im}(Z) \neq 0$. These instability domains are in the $\alpha < 1$ and $\alpha > 1$ regions. With increasing β the left instability domain becomes narrow and is shifted to the point $\alpha = 1$. The right domain is shifted from this point away to the right-hand sight. With further increase of β in the right domain the instability disappears, $\text{Im}(Z) \to 0$. For large values of β ($\beta \gg 1$ for $\alpha < 1$ and $\beta \gg \alpha^2$ for $\alpha > 1$) the first solution of

$Z = \pm\zeta_1^{1/2}$ passes to the solution (32), which is the prototype of Alfvén waves. The reason is that for such large β we get $\text{Re}(s_1) \approx \text{Re}(s_2)$ and $\text{Im}(s_1) \approx -\text{Im}(s_2)$, so $\zeta_1 < 0$ and $\zeta_{2,3} > 0$. In the subsequent section we investigate the dependence of the parameters determining the conditions for the appearance of the instability. For the present case $\gamma = 0$ this condition is Eq. (41) which describes the points of $\text{Im}(Z) = 0$ in Figs. 5.

4.3. Highly anisotropic wave propagation

The more realistic case $\gamma \gg 1$ is also of interest. We have already seen that for large β values $\gamma \neq 0$ makes the wave propagation velocities strongly anisotropic with respect to the magnetic field direction. In the limit $\gamma \gg 1$ we have the following asymptotic solutions of Eq. (31):

$$Z \approx Z_0 - \frac{c_6 Z_0^6 + c_4 Z_0^4 + c_2 Z_0^2 + c_0}{2Z_0^2(2c_5 Z_0^2 + c_3)},$$

$$Z_0^2 = \frac{-c_3 \pm \sqrt{c_3^2 - 4c_1 c_5}}{2c_5} \qquad (38)$$

The four asymptotic solutions, which are included in Eqs. (38), are symmetric with respect to the phase velocities, but they are highly unstable. Some characteristic pictures for the instability growing rates of these solutions are shown in Figs. 6. It is seen that with increasing γ the instability areas are shifted to the region $\alpha > 2$.

The remaining two solutions of Eq. (31) describe stable, but highly anisotropic modes with slow and high phase velocities:

$$Z_5 \approx -\frac{c_0}{c_1} - \left(\frac{c_0}{c_1}\right)^2 \frac{c_1 c_2 - c_0 c_3}{c_1^2},$$

$$Z_6 \approx -\frac{c_5}{c_6} + \frac{c_4 c_5 - c_3 c_6}{c_5^2} \qquad (39)$$

These asymptotic solutions can be used for moderate values of β. In the limit $\gamma \approx \beta \gg 1$ we have four stable and two unstable solutions. We consider here only complex solutions describing instability:

$$Z \approx \pm i\sqrt{\beta\frac{\alpha - 2}{\alpha l_2 - l_1(\alpha - 2)}} \qquad (40)$$

In this case the instability range is $2 < \alpha < 2l_1/(l_1 - l_2)$. This condition is obeyed only for the propagation angles $0 < \phi \leq \frac{\pi}{4}$.

The asymptotic solutions which are valid for large γ are in good agreement with the exact numerical solutions of Eq. (31). They can simply be handled.

5. Domains of instability

The coefficients $c_1 \ldots c_6$ of Eq. (31) are real functions of the magnetic field parameter β, of the anisotropy parameter α, of the thermal flux parameter γ, and of

the wave propagation angle ϕ. In dependence on these parameters the solution $Z(\alpha, \beta, \gamma, \phi)$ can become complex, otherwise an instability will arise. Formally in this case an exponential damping and a growing of the wave amplitudes exist at the same time. This is because the nonzero imaginary part of the solution of Eq. (31) has both signs. In the Appendix we derive analytically the general condition for which the instability can exist. The parametric equation $D(\alpha, \beta, \gamma, \phi) = 0$ in Eq. (A.5) (See: Appendix) defines the boundaries of the instability domain. If thermal fluxes are absent which is fitted by the limit case $\gamma = 0$, Eq. (A.5) is drastically simplified.

We have
$$\alpha = 1, \; 2c_6 = \alpha(1 + l_1) - 2l_1 = 0,$$
and
$$D_0 = 27c_0^2 c_6^2 + 2c_0 c_4 \left(2c_4^2 - 9c_2 c_6\right) + c_2^2 \left(4c_2 c_6 - c_4^2\right) = 0. \quad (41)$$

In the instability domains D > 0. This idealized case is shown in Figs. 7. Instability areas are labeled by the sign "+". The line $\alpha = 1$ divides the areas into two parts. With increasing β the instability disappears. The differences of these results from the corresponding results of Baranov and Krasnobayev [31] and, Kuznetsov and Oraevskii [33] are probably due to the more general equations which we are using here.

A physically more interesting range of parameters with $\gamma \neq 0$ for the instability areas is also shown in Figs. 7. In this case all conditions are more complicated. For the given set of parameters we can get one, two, or all three pairs of complex solutions. The condition Eq. (A.5) includes all of these situations. Every point in these curves corresponds to the boundary of the instability domain. The thermal flux case $\gamma \neq 0$ make the areas very complicated, especially for strong magnetic fields, $\beta >> 1$. All the increments or instability rate regions shown in the pictures above as examples are described by the general Eq. (A.5).

6. Concluding remarks

Our approach has been motivated by earlier and recent coronal spectral line observations, which suggest that the following three unresolved coronal physics problems have probably a common origin:

i) a broadening of coronal line profiles due to some permanent turbulent motions, which exist globally everywhere;

ii) the sources of coronal heating are independent from the magnetic activity phase and to a minor extent from the magnetic configurations;

iii) the particle acceleration and the solar wind problems seem to have the same origin.

We prefer here the idea of the wave mechanism. In spite of so much theoretical efforts based on the isotropic MHD equations, the problems remained unsolved. The usual MHD equations are derived assuming that the plasma is still collision-dominated and the gas pressure is isotropic. However, this approximation cannot work satisfactory in a rarefied hot magnetized plasma.

Of course, the best way is the use of the kinetic Boltzmann-Vlasov equations avoiding usual MHD.

However, the solution of these nonlinear integro-differential equations written for each plasma component in the 6-dimensional phase space of (u, r) is extremely difficult. Besides, we are not interested in any small-scale plasma wave turbulence. We have to study the plasma motions integrated over large space and time scales (this is done by applying the MHD equations in usual cases). For this aim we use the 16–moments transport equations, derived as integrated moments of the kinetic equations. In earlier similar attempts the 13–moments equations have been used. However, these equations without any motivations exclude the appearance of the thermal fluxes and they are therefore incomplete.

Anisotropy is the main feature of a collisionless plasma with a strong magnetic field ($\lambda_{e,i} >> r_B$). Within large enough time intervals, t → ∞, both the electron and the ion components of the plasma tend to reach a steady Maxwellian distribution. If there would be no external magnetic field, an isotropic state would be reached. However, the magnetic field results in non-uniform distributions of speeds, $u_\parallel \neq u_\perp$, that leads to an anisotropy in the impulses of particles. In the present study the pressure anisotropy is described by the parameter α and heat fluxes by γ. Taking $\gamma = 0$ we do no pass to the 13–moments equations, or taking $\alpha = 1$ and $\gamma = 0$ we do no pass to the isotropic MHD case. The 16–moments equations are in principle different equations. Using these equations we have shown that a wide unstable and stable wave spectrum in the collisionless anisotropy plasma is possible, even in the incompressible approximation. If $\gamma \neq 0$ (heat fluxes are present) the waves run along and against the magnetic field with different speeds. This behavior is different from the usual isotropic MHD case. This spectrum range is strongly dependent on the magnetic field value (parameter β), on the pressure anisotropy parameter α, on the heat fluxes parameter γ, and on the wave propagation angle ϕ with respect to the magnetic field. The deduced instability increments are rather large. We have obtained the general instability condition.

Let us consider some example of the instability growing time for coronal values. In accordance with observations it is probable that the ions (protons and heavy ions) are heated more strongly in the direction across the magnetic field than along it: $T_\perp / T_\parallel = \Lambda > 1$. Some observations of the solar wind (see, e.g., Marsch [20]) detected an electron temperature anisotropy with an opposite relation: $T_{e\parallel} > T_{e\perp}$. In the corona the ion temperature anisotropy results in an anisotropy of the partial gas pressure and thus of the total pressure, $p = p_e + p_i$. If we take $n_e \approx n_i$ and $p \approx n_e k (T_e + T_i)$, then $\alpha = p_\perp / p_\parallel \approx (T_e + T_\perp)/(T_e + T_\parallel)$. To estimate α we should know the relation between T_e and $T_{\perp, \parallel}$.

Four cases should be considered:
1) $T_e \approx T_\parallel$ and then $\alpha = (1 + \Lambda)/2 > 0.5$;

2) $T_e \approx T_\perp$ and then $\alpha = 2\Lambda/(1+\Lambda) < 2$;

3) $T_e \approx (T_\perp + T_\parallel)/2$ and then $\alpha = (1+3\Lambda)/(3+\Lambda)$, where $0.33 < \alpha < 3$;

4) $T_e \approx \sqrt{(T^2_\perp + T^2_\parallel)/2}$

and $\alpha = \left(\sqrt{1+\Lambda^2} + \sqrt{2}\Lambda\right)/\left(\sqrt{1+\Lambda^2} + \sqrt{2}\right)$,

where $\left(1+\sqrt{2}\right)^{-1} < \alpha < \left(1+\sqrt{2}\right)$.

The first version is perhaps the most probable one. In any case let us take α = 1.5. Let also B$_0$ = 3G and T$_e$ = 10^6 K. Then $\beta \approx 10$ and $c_\parallel \approx c_s \sim 100$ km s^{-1}. We assume $v_0 \sim c_\parallel$ and then $\gamma \sim 1$. So from Figs. 2 we see that for such parameters $d \approx 0.3$ and $V_{ph} \sim 1$. $d \approx 0.3$ means that $P_w/t_{ins} \sim 2$, where P_w is the wave period, and t$_{ins}$ is the characteristic growing time. For P$_w \sim 5$ min we have a transverse wavelength of $\lambda \sim 10^3$ km. These estimates belong to the oscillation range observed in coronal loops [7] (see Section 1). Quickly growing modes will likely disappear due to nonlinear dissipation.

In a collisionless approach under the influence of an external magnetic field we should, strictly speaking, consider the equations for four different temperatures, $T_\parallel \neq T_\perp$ and $T_e \neq T_i$. However, on real conditions the relaxation time of particles is small enough, $\tau_{e,i} \ll \tau$. Thus, the balance between ion and electron temperatures is quickly restored, and the anisotropic temperatures with respect to the magnetic field become more important.

In subsequent studies the present work should be extended to the compressible case and to the consideration of radiative losses, such as it has been done by Somov et al [36] for isotropic MHD.

Acknowledgement

Appendix A: Dependence of the instability domains on the parameters

Let us consider a polynomial equation of degree N with real coefficients c_N:

$$P = \sum_{n=0}^{N} c_n Z^n = 0 \tag{A.1}$$

Here the coefficients are functions of several parameters, say α, β, γ and ϕ. Physically instability is possible only if the solutions become complex, because Z is a dimensionless wave frequency. As the coefficients are real the complex solutions of Eq. (A.1) are conjugated: $Z = x \pm iy$. For x and y we have two equations:

$$f_1 = \mathrm{Re}(P) = 0, \quad f_2 = \frac{1}{y}\mathrm{Im}(P) = 0 \tag{A.2}$$

where $f_1 = f_1(c_j; x; y)$, $f_2 = f_2(c_j; x; y)$. The boundaries of the instability domains are defined by the equations $f_1(c_j; x; 0) = 0$ and $f_2(c_j; x; 0) = 0$. So we get from Eq. (A.1) the following two equations:

$$\sum_{n=0}^{N} c_n x^n = 0, \quad \sum_{n=0}^{N} n c_n x^{n-1} = 0 \tag{A.3}$$

To verify this statement let us first test the quadratic equation case: $N = 2$. In this case Eq. (A.1) has two solutions: $2c_2 Z = -c_1 \pm \sqrt{c_1^2 - 4c_0 c_2}$. The instability appears if the condition $c_1^2 < 4c_0 c_2$ is fulfilled. In this case the boundaries of the domain of instability are given by the parametric equation $D(\alpha, \beta, \gamma, \phi) = c_1^2 - 4c_0 c_2 = 0$. For this sample Eqs.(A.3) are $c_0 + c_1 x + c_2 x^2 = 0, \quad c_1 + 2c_2 x = 0$

Excluding here the variable x we can get the same domain equation $D(\alpha, \beta, \gamma, \phi) = 0$.

The same procedure can be applied to the more general case when N is an arbitrary number. For our 6 th-order wave dispersion Eq. (31) $N = 6$. If we exclude x from Eqs. (A.3) in this case we receive the necessary condition for the wave instability.

Let us take $d_j = (1 - j/6)c_j$, $j = 0,...,6$,

$$m_1 = d_4 - d_5 \frac{5c_5}{6c_6}; \quad m_2 = 5c_5 + \frac{6c_6}{m_1}\left(d_5 \frac{4c_4}{6c_6} - d_3\right),$$

$$m_3 = \frac{m_2}{m_1}\left(d_5 \frac{4c_4}{6c_6} - d_3\right) + \frac{6c_6}{m_1}\left(d_5 \frac{3c_3}{6c_6} - d_2\right) + 4c_4,$$

$$r_0 = \frac{m_2}{m_1}\left(d_5 \frac{c_1}{6c_6} - d_0\right) + c_1, \quad m_4 = r_2 \frac{m_1}{m_3} + d_5 \frac{4c_4}{6c_6} - d_3,$$

$$r_1 = \frac{m_2}{m_1}\left(d_5 \frac{2c_2}{6c_6} - d_1\right) + \frac{6c_6}{m_1}\left(d_5 \frac{c_1}{6c_6} - c_0\right) + 2c_2,$$

$$r_2 = \frac{m_2}{m_1}\left(d_5 \frac{3c_3}{6c_6} - d_2\right) + \frac{6c_6}{m_1}\left(d_5 \frac{2c_2}{6c_6} - d_1\right) + 3c_3,$$

$$s_0 = r_0 \frac{m_4}{m_3} - d_5 \frac{c_1}{6c_6} + c_0,$$

$$s_1 = r_1 \frac{m_4}{m_3} - r_0 \frac{m_1}{m_3} - d_5 \frac{2c_2}{6c_6} + d_1,$$

$$s_2 = r_2 \frac{m_4}{m_3} - r_1 \frac{m_1}{m_3} - d_5 \frac{3c_3}{6c_6} + d_2,$$

$$s_3 = r_1 - m_3 \frac{s_0}{s_2} - \frac{s_1}{s_2}\left(r_2 - m_3 \frac{s_1}{s_2}\right),$$

$$s_4 = r_0 - \frac{s_0}{s_2}\left(r_2 - m_3 \frac{s_1}{s_2}\right). \tag{A.4}$$

Then we have the final parametric equation for boundaries of the instability domain to be determined:

$$D(\alpha, \beta, \gamma, \phi) = s_2\left(\frac{s_4}{s_3}\right)^2 - s_1 \frac{s_4}{s_3} + s_0 = 0 \tag{A.5}$$

References

[1] W.Grotrian, "Sonne und Ionosphare", Naturwiss., v.27, 1939, pp.555-577.

[2] B.Edl´en, P. Swings, "Term Analysis of the Third Spectrum of Iron (Fe III)", Ap.J., v.95, 1942, pp.532-539.

[3] L.Biermann, "Oszillatorenstarken in verschiedenen Grenzkontinuen in den Spektren von Mg II und Si II", Naturwiss., v. 33, 1946, pp.118-119.

[4] G.B.Parker, "Topological Dissipation and the Small-Scale Fields in Turbulent Gases', Ap.J., v.174, 1972, pp.499-504.

[5] G.B.Parker, "Magnetic Neutral Sheets in Evolving Fields - Part Two - Formation of the Solar Corona", Ap.J., v. 264, 1983, pp.642-649.

[6] M.J.Aschwanden, A.Winebarger, D.Tsiklauri, H.Peter, "The Coronal Heating Paradox", Ap.J., v.659, 2007, pp.1673-1681.

[7] M.J.Aschwanden, "Physics of the Solar Corona. An Introduction with Problems and Solutions" (2nd edition), Springer, 2005, p.892.

[8] M.J.Aschwanden, R.W.Nightingale, J.Andries, M.Goossens, T. Van Doorsselare, "Observational Tests of Damping by Resonant Absorption in Coronal Loop Oscillations", Ap.J., v. 598, 2003, pp.1375-1386.

[9] J.Heyvaerts, Asymptotic structure of MHD winds and jets, Astronomical and Astrophysical Transactions, v. 20, Issue 2, pp.295-302.

[10] W.C.Feldman, J.A.Asbridge, S.J.Bame, M.D.Montgomery, "Interpenetrating solar wind streams", Rev. Geophys. Space Phys., v. 12, 1974, pp.715-723.

[11] E.Marsch, K.-H.Muhlhauser, R.Schwen, H.Rosenbauer, W.G.Pilipp, F.M.Neubauer, "Solar wind protons - Three-dimensional velocity distributions and derived plasma parameters measured between 0.3 and 1 AU", J. Geophys. Res., v.87, 1982, pp.52-72.

[12] J.C.Casper, A.J.Lazarus, S.P.Gary, A.Szabo, in: "Solar Wind Ten", M.Velli, R.Bruno, and F.Malara (Eds.), Proc. 10th Intern. Solar Wind Conference, Pisa, Italy, 12-21 June 2002, AIP Conf. Proc., v.679, 2003, p.538.

[13] D.H.Clark, W.J.Raitt, A.P.Willmore, "A measured anisotropy in the ionospheric electron temperature", J. Atmos. Terr. Phys., v.35, 1973, pp.63-67.

[14] Ja.I.Likhter, V.I.Larkina, Yu.M.Mikhailov, et.al. Space Res., v.19, 1979, p.339.

[15] J. L.Kohl, G.Noci, E.Antonucci, and 28 coauthors, "UVCS/SOHO Empirical Determinations of Anisotropic Velocity Distributions in the Solar Corona", Ap.J., v.501, 1998, L127-L129.

[16] S.R.Cranmer, J.L.Kohl, G.Noci, and 28 coauthors, "An Empirical Model of a Polar Coronal Hole at Solar Minimum", Ap.J., v.511, 1999, pp.481-501.

[17] M.A.Dodero, E.Antonucci, S.Giordano, R.Martin, "Solar Wind Velocity and Anisotropic Coronal Kinetic Temperature Measured with the O VI Doublet Ratio", Sol. Phys., v.183, 1998, pp.77-90.

[18] E.Antonucci, M.A.Dodero, S.Giordano, "Fast Solar Wind Velocity in a Polar Coronal Hole during Solar Minimum", Sol. Phys., v.197, 2000, pp.115-134.

[19] J.V.Hollweg, P.A.Isenberg, "Generation of the fast solar wind: A review with emphasis on the resonant cyclotron interaction', J. Geophys. Res., v.107, 2002, pp.1147-1155.

[20] E.Marsch, "Kinetic Physics of the Solar Corona and Solar Wind", Living Rev. Solar Phys., v.3, 2006, p.1.

[21] V.N.Oraevskii, Y.V.Konikov, G.V.Chazanov, "Transport Processes in Anisotropic Near-Earth Plasma", Moscow, Nauka, 1985, p.173.

[22] A.I.Achieser, "Electrodynamics of Plasma", Moscow, Nauka, 1974, p.719.

[23] G.F.Chew, M.L.Goldberger, F.E.Low, "The Boltzmann Equation and the One-Fluid Hydromagnetic Equations in the Absence of Particle Collisions", Proc. Roy. Soc. London A, v.236, 1956, p.112.

[24] L.I.Rudakov, R.Z.Sagdeev, in: "The Plasma Physics and Problems of Controlling Nuclear Reaction", Moscow, v.3, 1958, p.268.

[25] H.Grad, Commun. Pure and Appl. Math., v. 2, 1949, p.331.

[26] V.Oraevskii, R.Chodura, W.Feneberg, Hydrodynamic equations for plasmas in strong magnetic fields - I: Collisionless approximation Plasma Phys., v.10, 1968, pp.819-828.

[27] H.G.Demars, R.W.Schunk, "Transport equations for multispecies plasmas based on individual bi-Maxwellian distributions", J. Phys. D, v.12, 1979, pp.1051-1077.

[28] E.L.Olsen, E.Leer, "A study of solar wind acceleration based on gyrotropic transport equations", J. Geophys. Res., v.104, 1999, pp.9963-9972.

[29] X.Li, "Proton temperature anisotropy in the fast solar wind: A 16-moment bi-Maxwellian model", J. Geophys. Res., v.104, 1999, pp.19773-19786.

[30] O.Lie-Svendsen, E.Leer, V.H.Hasteen, "A 16-moment solar wind model: From the chromosphere to 1 AU", J. Geophys. Res., v.106, 2001, pp.8217-8232.

[31] V.B.Baranov, K.V.Krasnobayev, "Hydrodynamics of Cosmic Plasma", Moscow, Nauka, 1977, p.335.

[32] Y.Kato, M.Tajiri, T.Taniuti, "Propagation of Hydromagnetic Waves in Collisionless Plasma, I", J. Phys. Soc. Japan, v.21, 1966, pp.765-771.

[33] V.D.Kuznetsov, V.N.Oraevskii, Astron. Lett., v.18, 1992, p.547.

[34] J.V.Hollweg, "On electron heat conduction in the solar wind", J. Geophys. Res., v.79, 1974, pp.3845-3850.

[35] J.V.Hollweg, "Collisionless electron heat conduction in the solar wind", J. Geophys. Res., v.81, 1976, pp.1649-1658.

[36] B.V.Somov, N.S.Dzhalilov, J.Staude, "Peculiarities of entropy and magnetosonic waves in optically thin cosmic plasma", Astron. Lett., v.33, 2007, pp.309-318.